



# Projections of oceanic N<sub>2</sub>O emissions in the 21st century using the IPSL Earth system model

J. Martinez-Rey<sup>1,a</sup>, L. Bopp<sup>1</sup>, M. Gehlen<sup>1</sup>, A. Tagliabue<sup>2</sup>, and N. Gruber<sup>3</sup>

<sup>1</sup>Laboratoire des Sciences du Climat et de l'Environnement, IPSL, CEA/CNRS/UVSQ, Bat. 712 – Orme des Merisiers, 91191 CE Saclay, Gif-sur-Yvette, France

<sup>2</sup>School of Environmental Sciences, University of Liverpool, 4 Brownlow Street, Liverpool L69 3GP, UK

<sup>3</sup>Environmental Physics, Institute of Biogeochemistry and Pollutant Dynamics, ETH, CHN E31.2, Universitaetstrasse 16, 8092 Zürich, Switzerland

<sup>a</sup>now at: Laboratoire des Sciences de l'Environnement Marin (LEMAR), UBO/CNRS/IRD/Ifremer, Institut Universitaire Européen de la Mer (IUEM), Technopole Brest Iroise, 29280, Plouzané, France

Correspondence to: J. Martinez-Rey (jorge.martinezrey@univ-brest.fr, jorge.martinez-rey@lsce.ipsl.fr)

Received: 16 September 2014 – Published in Biogeosciences Discuss.: 05 December 2014

Revised: 08 May 2015 – Accepted: 27 May 2015 – Published: 13 July 2015

**Abstract.** The ocean is a substantial source of nitrous oxide (N<sub>2</sub>O) to the atmosphere, but little is known about how this flux might change in the future. Here, we investigate the potential evolution of marine N<sub>2</sub>O emissions in the 21st century in response to anthropogenic climate change using the global ocean biogeochemical model NEMO-PISCES. Assuming nitrification as the dominant N<sub>2</sub>O formation pathway, we implemented two different parameterizations of N<sub>2</sub>O production which differ primarily under low-oxygen (O<sub>2</sub>) conditions. When forced with output from a climate model simulation run under the business-as-usual high-CO<sub>2</sub> concentration scenario (RCP8.5), our simulations suggest a decrease of 4 to 12 % in N<sub>2</sub>O emissions from 2005 to 2100, i.e., a reduction from 4.03/3.71 to 3.54/3.56 TgN yr<sup>-1</sup> depending on the parameterization. The emissions decrease strongly in the western basins of the Pacific and Atlantic oceans, while they tend to increase above the oxygen minimum zones (OMZs), i.e., in the eastern tropical Pacific and in the northern Indian Ocean. The reduction in N<sub>2</sub>O emissions is caused on the one hand by weakened nitrification as a consequence of reduced primary and export production, and on the other hand by stronger vertical stratification, which reduces the transport of N<sub>2</sub>O from the ocean interior to the ocean surface. The higher emissions over the OMZ are linked to an expansion of these zones under global warming, which leads to increased N<sub>2</sub>O production, associated primarily with denitrification. While there are many uncertainties in the relative contribution and

changes in the N<sub>2</sub>O production pathways, the increasing storage seems unequivocal and determines largely the decrease in N<sub>2</sub>O emissions in the future. From the perspective of a global climate system, the averaged feedback strength associated with the projected decrease in oceanic N<sub>2</sub>O emissions amounts to around  $-0.009 \text{ W m}^{-2} \text{ K}^{-1}$ , which is comparable to the potential increase from terrestrial N<sub>2</sub>O sources. However, the assessment for a potential balance between the terrestrial and marine feedbacks calls for an improved representation of N<sub>2</sub>O production terms in fully coupled next-generation Earth system models.

## 1 Introduction

Nitrous oxide (N<sub>2</sub>O) is a gaseous compound responsible for two key feedback mechanisms within the Earth's climate. First, it acts as a long-lived and powerful greenhouse gas (Prather et al., 2012) ranking third in anthropogenic radiative forcing after carbon dioxide (CO<sub>2</sub>) and methane (CH<sub>4</sub>) (Myhre et al., 2013). Secondly, the ozone (O<sub>3</sub>) layer depletion in the future might be driven mostly by N<sub>2</sub>O after the drastic reductions in CFCs emissions start to show their effect on stratospheric chlorine levels (Ravishankara et al., 2009). The atmospheric concentration of N<sub>2</sub>O is determined by the natural balance between sources from land and ocean and the destruction of N<sub>2</sub>O in the atmosphere largely by pho-

tolysis (Crutzen, 1970; Johnston, 1971). The natural sources from land and ocean amount to  $\sim 6.6$  and  $3.8 \text{ TgN yr}^{-1}$ , respectively (Ciais et al., 2013). Anthropogenic activities currently add an additional  $6.7 \text{ TgN yr}^{-1}$  to the atmosphere, which has caused atmospheric N<sub>2</sub>O to increase by 18 % since preindustrial times (Ciais et al., 2013), reaching 325 ppb in the year 2012 (NOAA ESRL Global Monitoring Division, Boulder, Colorado, USA, <http://esrl.noaa.gov/gmd/>).

Using a compilation of 60 000 surface ocean observations of the partial pressure of N<sub>2</sub>O ( $p\text{N}_2\text{O}$ ), Nevison et al. (2004) computed a global ocean source of  $4 \text{ TgN yr}^{-1}$ , with a large range of uncertainty from 1.2 to  $6.8 \text{ TgN yr}^{-1}$ . Model-derived estimates also differ widely, i.e., between 1.7 and  $8 \text{ TgN yr}^{-1}$  (Nevison et al., 2003; Suntharalingam et al., 2000). These large uncertainties are a consequence of too few observations and of poorly known N<sub>2</sub>O formation mechanisms, reflecting a general lack of understanding of key elements of the oceanic nitrogen cycle (Gruber and Galloway, 2008; Zehr and Ward, 2002), and of N<sub>2</sub>O in particular (e.g., Zamora et al., 2012; Bange et al., 2009; Freing et al., 2012). A limited number of interior ocean N<sub>2</sub>O observations were made available only recently (Bange et al., 2009), but they contain large temporal and spatial gaps. Information on the rates of many important processes remains insufficient, particularly in natural settings. There are only a few studies from a limited number of specific regions such as the Arabian Sea, central and North Pacific, Black Sea, the Bedford Basin and the Scheldt estuary, which can be used to derive and test model parameterizations (Mantoura et al., 1993; Bange et al., 2000; Elkins et al., 1978; Farias et al., 2007; Frame and Casciotti, 2010; Westley et al., 2006; Yoshida et al., 1989; Punshon and Moore, 2004; de Wilde and de Bie, 2000).

N<sub>2</sub>O is formed in the ocean interior through two major pathways and consumed only in oxygen minimum zones (OMZs) through denitrification (Zamora et al., 2012). The first production pathway is associated with nitrification (conversion of ammonia,  $\text{NH}_4^+$ , into nitrate,  $\text{NO}_3^-$ ), and occurs when dissolved O<sub>2</sub> concentrations are above  $20 \mu\text{mol L}^{-1}$ . We subsequently refer to this pathway as the high-O<sub>2</sub> pathway. The second production pathway is associated with a series of processes when O<sub>2</sub> concentrations fall below  $\sim 5 \mu\text{mol L}^{-1}$  and involves a combination of nitrification and denitrification (hereinafter referred to as low-O<sub>2</sub> pathway) (Cohen and Gordon, 1978; Goreau et al., 1980; Elkins et al., 1978). As nitrification is one of the processes involved in the aerobic remineralization of organic matter, it occurs nearly everywhere in the global ocean with a global rate at least one order of magnitude larger than the global rate of water column denitrification (Gruber, 2008). One of the main reasons is that denitrification in the water column is limited to the OMZs, which occupy only a few percent of the total ocean volume (Bianchi et al., 2012). This is also the only place in the water column where N<sub>2</sub>O is being consumed.

The two production pathways have very different N<sub>2</sub>O yields, i.e., fractions of nitrogen-bearing products that are transformed to N<sub>2</sub>O. For the high-O<sub>2</sub> pathway, the yield is typically rather low, i.e., only about one in several hundred molecules of ammonium escapes as N<sub>2</sub>O (Cohen and Gordon, 1979). In contrast, in the low-O<sub>2</sub> pathway, and particularly during denitrification, this fraction may go up to as high as 1 : 1, i.e., that all nitrate is turned into N<sub>2</sub>O (Tiedje, 1988). The relative contribution of the two pathways to global N<sub>2</sub>O production is not well established. Sarmiento and Gruber (2006) suggested that the two may be of equal importance, but more recent estimates suggest that the high-O<sub>2</sub> production pathway dominates global oceanic N<sub>2</sub>O production (Freing et al., 2012).

Two strategies have been pursued in the development of parameterizations for N<sub>2</sub>O production in global biogeochemical models. The first approach builds on the importance of the nitrification pathway and its close association with the aerobic remineralization of organic matter. As a result the production of N<sub>2</sub>O and the consumption of O<sub>2</sub> are closely tied to each other, leading to a strong correlation between the concentration of N<sub>2</sub>O and the apparent oxygen utilization (AOU). This has led to the development of two sets of parameterizations, one based on concentrations, i.e., directly as a function of AOU (Butler et al., 1989), and the other based on the rate of oxygen utilization, i.e., OUR (Freing et al., 2009). Additional variables have been introduced to allow for differences in the yield, i.e., the ratio of N<sub>2</sub>O produced over oxygen consumed, such as temperature (Butler et al., 1989) or depth (Freing et al., 2009). In the second approach, the formation of N<sub>2</sub>O is modeled more mechanistically and tied to both nitrification and denitrification by an O<sub>2</sub>-dependent yield (Suntharalingam and Sarmiento, 2000; Nevison et al., 2003; Jin and Gruber, 2003). Since most models do not include nitrification explicitly, the formation rate is actually coupled directly to the remineralization of organic matter. Regardless of the employed strategy, all parameterizations depend to first order on the amount of organic matter that is being remineralized in the ocean interior, which is governed by the export of organic carbon to depth. The dependence of N<sub>2</sub>O production on oxygen levels and on other parameters such as temperature plays a secondary role. This has important implications not only for the modeling of the present-day distribution of N<sub>2</sub>O in the ocean but also for the sensitivity of marine N<sub>2</sub>O to future climate change.

Over this century, climate change will perturb marine N<sub>2</sub>O formation in multiple ways. Changes in productivity will drive changes in the export of organic matter to the ocean interior (Steinacher et al., 2010; Bopp et al., 2013) and hence affect the level of marine nitrification. Ocean warming might change the rate of N<sub>2</sub>O production during nitrification (Freing et al., 2012). Changes in carbonate chemistry (Bindoff et al., 2007) might cause changes in the C : N ratio of the exported organic matter (Riebesell et al., 2007), altering not only the rates of nitrification but also the ocean interior oxy-

gen levels (Gehlen et al., 2011). Finally, the expected general loss of oxygen (Keeling et al., 2010; Cocco et al., 2013; Bopp et al., 2013) could substantially affect N<sub>2</sub>O production via both nitrifier denitrification and classic denitrification.

Ocean biogeochemical models used for IPCC's Fourth Assessment Report estimated a decrease between 2 and 13 % in primary production (PP) under the business-as-usual high-CO<sub>2</sub> concentration scenario A2 (Steinacher et al., 2010). A more recent multi-model analysis based on the models used in IPCC's Fifth Assessment Report also suggests a large reduction of PP down to 18 % by 2100 for the RCP8.5 scenario (Bopp et al., 2013). In these simulations, the export of organic matter is projected to decrease between 6 and 18 % in 2100 (Bopp et al., 2013), with a spatially distinct pattern: in general, productivity and export are projected to decrease at mid- to low latitudes in all basins, while productivity and export are projected to increase in the high latitudes and in the South Pacific subtropical gyre (Bopp et al., 2013). A wider spectrum of responses was reported regarding changes in the ocean oxygen content. While all models simulate decreased oxygen concentrations in response to anthropogenic climate change (by about 2 to 4 % in 2100), and particularly in the mid-latitude thermocline regions, no agreement exists with regard to the hypoxic regions, i.e., those having oxygen levels below 60 and 5  $\mu\text{mol L}^{-1}$  (Cocco et al., 2013; Bopp et al., 2013). Some models project these regions to expand, while others project a contraction. Even more divergence in the results exists for the suboxic regions, i.e., those having O<sub>2</sub> concentrations below 5  $\mu\text{mol L}^{-1}$  (Keeling et al., 2010; Deutsch et al., 2011; Cocco et al., 2013; Bopp et al., 2013), although the trend for most models is pointing towards an expansion. At the same time, practically none of the models is able to correctly simulate the current distribution of oxygen in the OMZ (Bopp et al., 2013). In summary, while it is clear that major changes in ocean biogeochemistry are looming ahead (Gruber, 2011), with substantial impacts on the production and emission of N<sub>2</sub>O, our ability to project these changes with confidence is limited.

In this study, we explore the implications of these future changes in ocean physics and biogeochemistry on the marine N<sub>2</sub>O cycle, and make projections of the oceanic N<sub>2</sub>O emissions from year 2005 to 2100 under the high-CO<sub>2</sub> concentration scenario RCP8.5. We analyze how changes in biogeochemical and physical processes such as net primary production (NPP), export production and vertical stratification in this century translate into changes in oceanic N<sub>2</sub>O emissions to the atmosphere. To this end, we use the NEMO-PISCES ocean biogeochemical model, which we have augmented with two different N<sub>2</sub>O parameterizations, permitting us to evaluate changes in the marine N<sub>2</sub>O cycle at the process level, especially with regard to production pathways in high- and low-oxygen regimes. We demonstrate that while future changes in the marine N<sub>2</sub>O cycle will be substantial, the net emissions of N<sub>2</sub>O appear to change relatively little – i.e., they are projected to decrease by about 10 % in 2100.

## 2 Methodology

### 2.1 NEMO-PISCES model

Future projections of the changes in the oceanic N<sub>2</sub>O cycle were performed using the PISCES ocean biogeochemical model (Aumont and Bopp, 2006) in offline mode with physical forcings derived from the IPSL-CM5A-LR coupled model (Dufresne et al., 2013). The horizontal resolution of NEMO ocean general circulation model is  $2^\circ \times 2^\circ \cos \varnothing$  ( $\varnothing$  being the latitude) with enhanced latitudinal resolution at the Equator of  $0.5^\circ$ . PISCES is a biogeochemical model with five nutrients (NO<sub>3</sub>, NH<sub>4</sub>, PO<sub>4</sub>, Si and Fe), two phytoplankton groups (diatoms and nanophytoplankton), two zooplankton groups (micro- and mesozooplankton) and two non-living compartments (particulate and dissolved organic matter). Phytoplankton growth is limited by nutrient availability and light. Constant Redfield C : N : P ratios of 122 : 16 : 1 are assumed (Takahashi et al., 1985), while all other ratios, i.e., those associated with chlorophyll, iron and silicon (Chl : C, Fe : C and Si : C), vary dynamically.

### 2.2 N<sub>2</sub>O parameterizations in PISCES

We implemented two different parameterizations of N<sub>2</sub>O production in NEMO-PISCES. The first one, adapted from Butler et al. (1989), follows the oxygen consumption approach, with a temperature-dependent modification of the N<sub>2</sub>O yield (P.TEMP). The second one is based on Jin and Gruber (2003) (P.OMZ), following the more mechanistic approach, i.e., it considers the different processes occurring at differing oxygen concentrations in a more explicit manner.

The P.TEMP parameterization assumes that the N<sub>2</sub>O production is tied to nitrification only. This is implemented in the model by tying the N<sub>2</sub>O formation in a linear manner to O<sub>2</sub> consumption. A small temperature dependence is added to the yield to reflect the potential impact of temperature on metabolic rates. The production term of N<sub>2</sub>O, i.e.,  $J^{\text{P.TEMP}}(\text{N}_2\text{O})$ , is then mathematically formulated as

$$J^{\text{P.TEMP}}(\text{N}_2\text{O}) = (\gamma + \theta T) J(\text{O}_2)_{\text{consumption}}, \quad (1)$$

where  $\gamma$  is a background yield ( $0.53 \times 10^{-4}$  mol N<sub>2</sub>O (mol O<sub>2</sub>)<sup>-1</sup> consumed),  $\theta$  is the temperature dependency of  $\gamma$  ( $4.6 \times 10^{-6}$  mol N<sub>2</sub>O (mol O<sub>2</sub>)<sup>-1</sup> K<sup>-1</sup>),  $T$  is temperature (K) and  $J(\text{O}_2)_{\text{consumption}}$  is the sum of all biological O<sub>2</sub> consumption terms within the model. The same ratio between constants  $\gamma$  and  $\theta$  is used in the model as in the original formulation from Butler et al. (1989). Although this parameterization is very simple, a recent analysis of N<sub>2</sub>O observations supports such an essentially constant yield, even in the OMZ of the eastern tropical Pacific (Zamora et al., 2012).

The P.OMZ parameterization, formulated after Jin and Gruber (2003), assumes that the overall yield consists of a constant background yield and an oxygen-dependent yield. The former is presumed to represent the N<sub>2</sub>O production by

nitrification, while the latter is presumed to reflect the enhanced production of N<sub>2</sub>O at low oxygen concentrations, in part driven by denitrification, but possibly including nitrification as well. This parameterization includes the consumption of N<sub>2</sub>O in suboxic conditions. This gives

$$J^{\text{P.OMZ}}(\text{N}_2\text{O}) = (\alpha + \beta f(\text{O}_2))J(\text{O}_2)_{\text{consumption}} - k\text{N}_2\text{O}, \quad (2)$$

where  $\alpha$  is, as in Eq. (1), a background yield ( $0.9 \times 10^{-4} \text{ mol N}_2\text{O} (\text{mol O}_2)^{-1}$  consumed);  $\beta$  is a yield parameter that scales the oxygen-dependent function ( $6.2 \times 10^{-4}$ );  $f(\text{O}_2)$  is a unitless oxygen-dependent step-like modulating function, as suggested by laboratory experiments (Goreau et al., 1980) (Fig. S1, Supplement); and  $k$  is the first-order rate constant of N<sub>2</sub>O consumption close to anoxia (zero otherwise). For  $k$ , we have adopted a value of  $0.138 \text{ yr}^{-1}$  following Bianchi et al. (2012) while we set the consumption regime for O<sub>2</sub> concentrations below  $5 \mu\text{mol L}^{-1}$ . The constant  $\alpha$  is on the same order of magnitude as the one proposed by Jin and Gruber (2003), while  $\beta$  is two orders of magnitude smaller. The use of the original value would result in a significant increase in N<sub>2</sub>O production associated with OMZs and, hence, in a departure from the assumption of dominant nitrification.

The P.OMZ parameterization allows us to independently quantify the N<sub>2</sub>O formation pathways associated with nitrification and those associated with low oxygen concentrations (nitrification/denitrification) and their evolution in time over the next century. Specifically, we consider the source term  $\alpha J(\text{O}_2)_{\text{consumption}}$  as that associated with the nitrification pathway, while we associated the source term  $\beta f(\text{O}_2) J(\text{O}_2)_{\text{consumption}}$  with the low-oxygen processes (Fig. S2, Supplement).

N<sub>2</sub>O production is inhibited by light in the model, and therefore N<sub>2</sub>O production in P.TEMP and P.OMZ parameterizations only occurs below a fixed depth of 100 m.

We employ a standard bulk approach for simulating the loss of N<sub>2</sub>O to the atmosphere via gas exchange. We use the formulation of Wanninkhof et al. (1992) for estimating the gas transfer velocity, adjusting the Schmidt number for N<sub>2</sub>O and using the solubility constants of N<sub>2</sub>O given by Weiss and Price (1980). We assume a constant atmospheric N<sub>2</sub>O concentration of 284 ppb in all simulations to explore future changes inherent to ocean processes without feedbacks due to changes in the atmosphere.

### 2.3 Experimental design

NEMO-PISCES was first spun up over 3000 years using constant preindustrial dynamical forcings fields from IPSL-CM5A-LR (Dufresne et al., 2013) without activating the N<sub>2</sub>O parameterizations. This spin-up phase was followed by a 150-year-long simulation, forced by the same dynamical fields now with N<sub>2</sub>O production and N<sub>2</sub>O sea-to-air flux embedded. The N<sub>2</sub>O concentration at all grid points was prescribed initially as  $20 \text{ nmol L}^{-1}$ , which is consistent with the

MEMENTO database average value of  $18 \text{ nmol L}^{-1}$  below 1500 m (Bange et al., 2009). During the 150-year spin-up, we diagnosed the total N<sub>2</sub>O production and N<sub>2</sub>O sea-to-air flux and adjusted the  $\alpha$ ,  $\beta$ ,  $\gamma$  and  $\theta$  parameters in order to achieve a total N<sub>2</sub>O sea-to-air flux in the two parameterizations at equilibrium close to  $3.85 \text{ Tg N yr}^{-1}$  (Ciais et al., 2013). In addition, the relative contribution of the high-O<sub>2</sub> pathway in the P.OMZ parameterization was set to 75 % of the total N<sub>2</sub>O production based on Suntharalingam et al. (2000), where a sensitivity model analysis on the relative contribution of high- and low-O<sub>2</sub> production pathways showed that a higher contribution of nitrification (75 %) than denitrification (25 %) achieved the best model performance compared to the data product from Nevison et al. (1995). P.TEMP can be considered as 100 % nitrification, testing in this way the hypothesis of nitrification as the dominant pathway of N<sub>2</sub>O production on a global scale. Nitrification could contribute with up to 93 % of the total production based on estimations considering N<sub>2</sub>O production along with water mass transport (Freing et al., 2012).

Projections in NEMO-PISCES of historical (from 1851 to 2005) and future (from 2005 to 2100) simulated periods were done using dynamical forcing fields from IPSL-CM5A-LR. These dynamical forcings were applied in an offline mode – i.e., monthly means of temperature, velocity, wind speed or radiative flux were used to force NEMO-PISCES. Future simulations used the business-as-usual high-CO<sub>2</sub> concentration scenario (RCP8.5) until year 2100. Century-scale model drifts for all the biogeochemical variables presented, including N<sub>2</sub>O sea-to-air flux, production and inventory, were removed using an additional control simulation with IPSL-CM5A-LR preindustrial dynamical forcing fields from year 1851 to 2100. Despite the fact that primary production and the export of organic matter to depth were stable in the control simulation, the air–sea N<sub>2</sub>O emissions drifted (an increase of 5 to 12 % in 200 years depending on the parameterization) due to the short spin-up phase (150 years) and the choice of the initial conditions for N<sub>2</sub>O concentrations.

## 3 Present-day oceanic N<sub>2</sub>O

### 3.1 Contemporary N<sub>2</sub>O fluxes

The model simulated air–sea N<sub>2</sub>O emissions show large spatial contrasts, with flux densities varying by one order of magnitude, but with relatively small differences between the two parameterizations (Fig. 1a and b). This is largely caused by our assumption that the dominant contribution (75 %) to the total N<sub>2</sub>O production in the P.OMZ parameterization is the nitrification pathway, which is then not so different from the P.TEMP parameterization, where it is 100 %. As a result, the major part of N<sub>2</sub>O is produced in the subsurface via nitrification, contributing directly to imprint changes into the

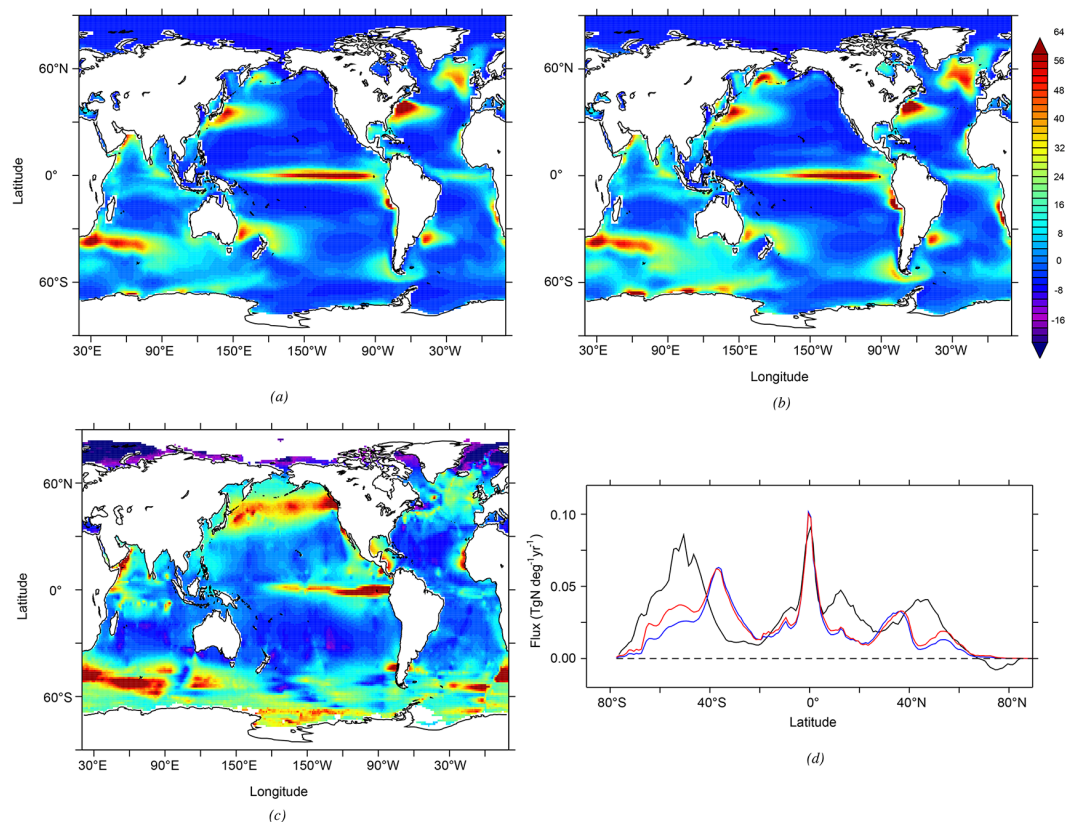


**Figure 1.** N<sub>2</sub>O sea-to-air flux (in  $\text{mgN m}^{-2} \text{yr}^{-1}$ ) from (a) P.TEMP parameterization averaged for the 1985 to 2005 time period in the historical simulation, (b) P.OMZ parameterization over the same time period, (c) data product of Nevison et al. (2004) and (d) latitudinal N<sub>2</sub>O sea-to-air flux (in  $\text{TgN deg}^{-1} \text{yr}^{-1}$ ) from Nevison et al. (2004) (black). P.TEMP: blue; P.OMZ: red.

sea-to-air N<sub>2</sub>O flux without significant meridional transport (Suntharalingam and Sarmiento, 2000).

Elevated N<sub>2</sub>O emission regions ( $> 50 \text{ mgN m}^{-2} \text{yr}^{-1}$ ) are found in the equatorial and eastern tropical Pacific, in the northern Indian ocean, in the northwestern Pacific, in the North Atlantic and in the Agulhas Current. In contrast, low fluxes ( $< 10 \text{ mgN m}^{-2} \text{yr}^{-1}$ ) are simulated in the Southern Ocean, Atlantic and Pacific subtropical gyres, and southern Indian Ocean. The large-scale distribution of N<sub>2</sub>O fluxes is coherent with Nevison et al. (2004) (Fig. 1c). This comes as a natural consequence of the relatively high contribution of nitrification, and hence hotspots of N<sub>2</sub>O emissions are associated with regions where higher export of organic matter occurs in the model.

There are, however, several discrepancies between the model and the data product. At high latitudes, the high N<sub>2</sub>O emissions observed in the North Pacific are not well represented in our model, with a significant shift towards the western part of the Pacific Basin, similar to other modeling studies (e.g., Goldstein et al., 2003; Jin and Gruber, 2003). The OMZ in the North Pacific, located at approximately 600 m deep, is underestimated in the model due to the deficient representation of the meridional overturning circulation (MOC)

in the North Pacific in global ocean biogeochemical models, which in turn might suppress areas of low oxygenation and therefore one potential N<sub>2</sub>O source. Discrepancies between model and observations also occur in the Southern Ocean, a region whose role in global N<sub>2</sub>O fluxes remains debated due to the lack of observations and the occurrence of potential artifacts due to interpolation techniques reflected in data products such as that from Nevison et al. (1995) (e.g., Suntharalingam and Sarmiento, 2000; Nevison et al., 2003). The model also overestimates N<sub>2</sub>O emissions in the North Atlantic. The emphasis put on the nitrification pathway suggests that hotspots of carbon export are at the origin of elevated concentrations of N<sub>2</sub>O in the subsurface. N<sub>2</sub>O is quickly outgassed to the atmosphere, leading to such areas of high N<sub>2</sub>O emissions in the model.

Model–data discrepancies can be seen as a function of latitude in Figure 1d. The modeled N<sub>2</sub>O flux maxima peak at around 40° S, i.e., around 10° north to that estimated by Nevison et al. (2004), although Southern Ocean data must be interpreted with caution. In the Northern Hemisphere the stripe in the North Pacific is not captured by the model, splitting the flux from the 45° N band into two peaks at 38 and 55° N.

**Table 1.** Standard deviation and correlation coefficients between P.TEMP and P.OMZ parameterizations with respect to MEMENTO database observations (Bange et al., 2009).

	P.TEMP	P.OMZ	OBS
Standard deviation (in nmol N <sub>2</sub> O L <sup>-1</sup> )	12	18	16
Correlation coefficient with obs.	0.49	0.42	–

### 3.2 Contemporary N<sub>2</sub>O concentrations and the relationship to O<sub>2</sub>

The model results at present day were evaluated against the MEMENTO database (Bange et al., 2009), which contains about 25 000 measurements of colocated N<sub>2</sub>O and dissolved O<sub>2</sub> concentrations. Table 1 summarizes the standard deviation and correlation coefficients for P.TEMP and P.OMZ compared to MEMENTO. The standard deviation of the model output is very similar to MEMENTO, i.e., around 16 nmol L<sup>-1</sup> of N<sub>2</sub>O. However, the correlation coefficients between the sampled data points from MEMENTO and P.TEMP/P.OMZ are 0.49 and 0.42, respectively. Largest discrepancies are found mostly in the deep ocean and in the OMZs.

Figure 2 compares the global average vertical profile of the observed N<sub>2</sub>O against the results from the two parameterizations. The in situ observations show three characteristic layers: the upper 100 m layer with low ( $\sim 10$  nmol L<sup>-1</sup>) N<sub>2</sub>O concentration due to gas exchange keeping N<sub>2</sub>O close to its saturation concentration, the mesopelagic layer, between 100 and 1500 m, where N<sub>2</sub>O is enriched via nitrification and denitrification in the OMZs, and the deep ocean beyond 1500 m, with a relatively constant concentration of 18 nmol L<sup>-1</sup> on average. Both parameterizations underestimate the N<sub>2</sub>O concentration in the upper 100 m, where most of the N<sub>2</sub>O is potentially outgassed to the atmosphere. In the second layer, P.OMZ shows a fairly good agreement with the observations in the 500 to 900 m band, whereas P.TEMP is too low by  $\sim 10$  nmol L<sup>-1</sup>. Below 1500 m, both parameterizations simulate too high N<sub>2</sub>O compared to the observations. This may be caused by the lack or underestimation of a sink process in the deep ocean, or by the too high concentrations used to initialize the model, which persist due to the rather short spin-up time of only 150 years.

The analysis of the model simulated N<sub>2</sub>O concentrations as a function of model simulated O<sub>2</sub> shows the differences between the two parameterizations more clearly (Fig. 3a and b). Such a plot allows us to assess the model performance with regard to N<sub>2</sub>O (Jin and Gruber, 2003), without being subject to the strong potential biases introduced by the model's deficiencies in simulating the distribution of O<sub>2</sub>. This is particularly critical in the OMZs, where all models exhibit strong biases (Cocco et al., 2013; Bopp et al., 2013). P.TEMP (Fig. 3a) slightly overestimates N<sub>2</sub>O for dissolved O<sub>2</sub> concentrations above 100  $\mu$ mol L<sup>-1</sup>, and does not

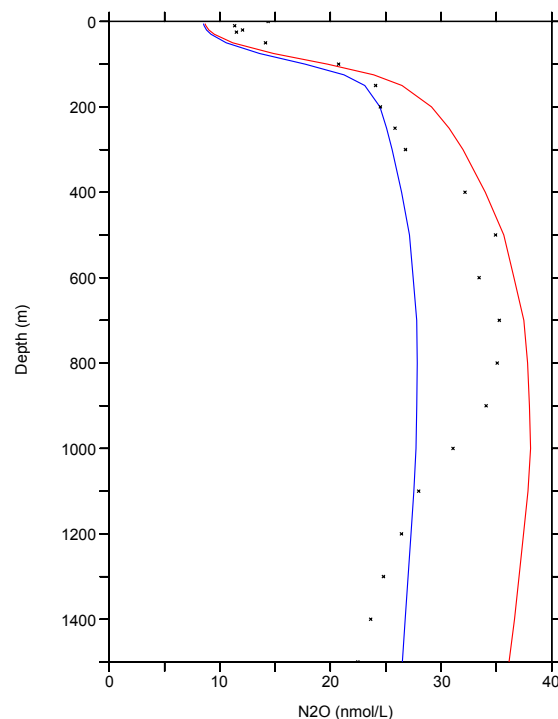


**Figure 2.** Global average depth profile of N<sub>2</sub>O concentration (in nmol L<sup>-1</sup>) from the MEMENTO database (dots) (Bange et al., 2009). P.TEMP: blue; P.OMZ: red. Model parameterizations are averaged over the 1985 to 2005 time period from the historical simulation.

fully reproduce either the high N<sub>2</sub>O values in the OMZs or the N<sub>2</sub>O depletion when O<sub>2</sub> is almost completely consumed. P.OMZ (Fig. 3b) overestimates the N<sub>2</sub>O concentration over the whole range of O<sub>2</sub>, with particularly high values of N<sub>2</sub>O above 100 nmol L<sup>-1</sup> due to the exponential function used in the OMZs. There, the observations suggest concentrations below 80 nmol L<sup>-1</sup> for the same low O<sub>2</sub> values, consistent with the linear trend observed for higher O<sub>2</sub>, which seems to govern over most of the O<sub>2</sub> spectrum, as suggested by Zamora et al. (2012). The discrepancy at low O<sub>2</sub> concentration may also stem from our choice of a too low N<sub>2</sub>O consumption rate under essentially anoxic conditions. Finally, it should be considered that most of the MEMENTO data points are from OMZs and therefore N<sub>2</sub>O measurements could be biased towards higher values than the actual open-ocean average, where our model performs better.

## 4 Future oceanic N<sub>2</sub>O

### 4.1 N<sub>2</sub>O sea-to-air flux

The global oceanic N<sub>2</sub>O emissions decrease relatively little over the next century (Fig. 4a) between 4 and 12%. That is, in P.TEMP, the emissions decrease by 0.15 from 3.71 TgN yr<sup>-1</sup> in 1985–2005 to 3.56 TgN yr<sup>-1</sup> in 2080–2100

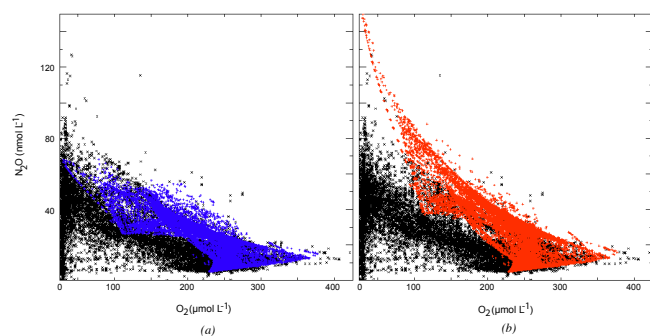


**Figure 3.** Relationship between O<sub>2</sub> concentration (in  $\mu\text{mol L}^{-1}$ ) and N<sub>2</sub>O concentration (in  $\text{nmol L}^{-1}$ ) in the MEMENTO database (black) (Bange et al., 2009), compared to model (a) P.TEMP (blue) and (b) P.OMZ (red) parameterizations averaged over the 1985 to 2005 time period from the historical simulation.

and in P.OMZ, the decrease is slightly larger at 12 %, i.e., amounting to  $0.49 \text{ Tg N yr}^{-1}$  from 4.03 to  $3.54 \text{ Tg N yr}^{-1}$ . Notable is also the presence of a negative trend in N<sub>2</sub>O emissions over the 20th century, most pronounced in the P.OMZ parameterization. Considering the change over the 20th and 21st centuries together, the model projects a decrease between 7 and 15 %.

These relatively small global decreases mask more substantial changes at the regional scale, with a mosaic of regions experiencing a substantial increase and regions experiencing a substantial decrease (Fig. 4b and c). In both parameterizations, the oceanic N<sub>2</sub>O emissions decrease in the northern and south western oceanic basins (e.g., the North Atlantic and Arabian seas) by up to  $25 \text{ mg N m}^{-2} \text{ yr}^{-1}$ . In contrast, the fluxes are simulated to increase in the eastern tropical Pacific and in the Bay of Bengal. For the Benguela Upwelling System (BUS) and the North Atlantic a bimodal pattern emerges in 2100. As was the case for the present-day distribution of the N<sub>2</sub>O fluxes, the overall similarity between the two parameterizations is a consequence of the dominance of the nitrification (high-O<sub>2</sub>) pathway in both parameterizations.

Nevertheless, there are two regions where more substantial differences between the two parameterizations emerge: the region overlying the oceanic OMZ at the BUS and the Southern Ocean. In particular, the P.TEMP parameterization projects a larger enhancement of the flux than P.OMZ at the BUS, whereas the emissions in the Southern Ocean are enhanced in the P.OMZ parameterization.

#### 4.2 Drivers of changes in N<sub>2</sub>O emissions

The changes in N<sub>2</sub>O emissions may stem from a change in net N<sub>2</sub>O production, a change in the transport of N<sub>2</sub>O from its location of production to the surface, or any combination of the two, which also includes changes in N<sub>2</sub>O storage. Next we determine the contribution of these mechanisms to the

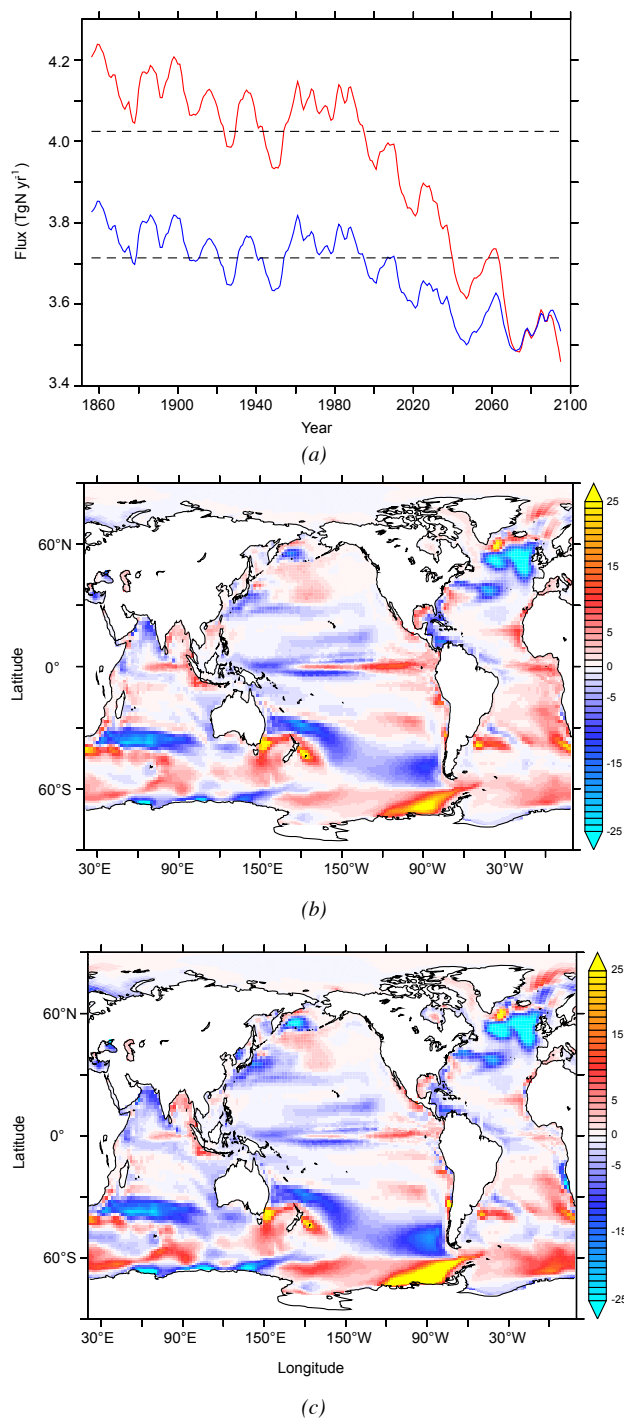


**Figure 4.** (a) N<sub>2</sub>O sea-to-air flux (in  $\text{Tg N yr}^{-1}$ ) from 1851 to 2100 in P.TEMP (blue) and P.OMZ (red) using the historical and future RCP8.5 simulations. Dashed lines indicate the mean value over the 1985 to 2005 time period. Change in N<sub>2</sub>O sea-to-air flux ( $\text{mg N m}^{-2} \text{ yr}^{-1}$ ) from the averaged 2080–2100 to 1985–2005 time periods in future RCP8.5 and historical simulations in (b) P.TEMP and (c) P.OMZ parameterizations.

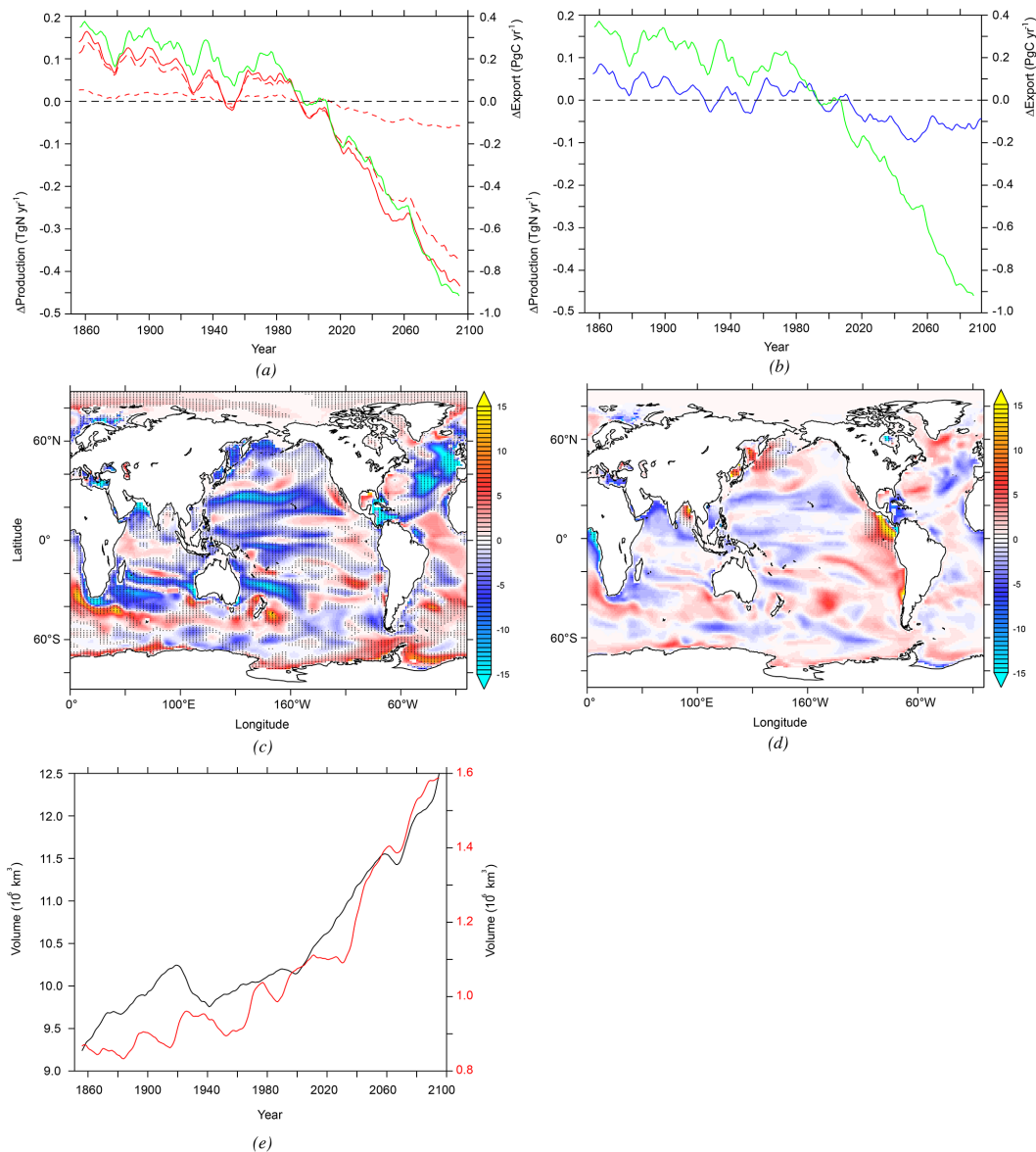


**Figure 5.** (a) Anomalies in export of organic matter at 100 m (green), low-O<sub>2</sub> production pathway (short dashed red), high-O<sub>2</sub> production pathway (long dashed red) and total P.OMZ production (red) from 1851 to 2100 using the historical and future RCP8.5 simulations. (b) Anomalies in export of organic matter at 100 m (green) and P. TEMP production (blue) over the same time period. (c) Change in high-O<sub>2</sub> production pathway of N<sub>2</sub>O (in mgN m<sup>-2</sup> yr<sup>-1</sup>) in the upper 1500 m between the 2080–2100 and 1985–2005 averaged time periods. Hatched areas indicate regions where change in export of organic matter at 100 m deep have the same sign as in changes in high-O<sub>2</sub> production pathway. (d) Change in low-O<sub>2</sub> production pathway of N<sub>2</sub>O (in mgN m<sup>-2</sup> yr<sup>-1</sup>) in the upper 1500 m between the 2080–2100 and 1985–2005 averaged time periods. Hatched areas indicate regions where oxygen minimum zones (O<sub>2</sub> < 5 μmol L<sup>-1</sup>) expand. (e) Volume (in 10<sup>6</sup> km<sup>3</sup>) of hypoxic (black, O<sub>2</sub> < 60 μmol L<sup>-1</sup>) and suboxic (red, O<sub>2</sub> < 5 μmol L<sup>-1</sup>) areas in the 1851 to 2100 period in NEMO-PISCES historical and future RCP8.5 simulations.

overall decrease in N<sub>2</sub>O emissions that our model simulated for the 21st century.

#### 4.2.1 Changes in N<sub>2</sub>O production

In both parameterizations, global N<sub>2</sub>O production is simulated to decrease over the 21st century. The total N<sub>2</sub>O pro-

duction in P.OMZ decreases by 0.41 TgN yr<sup>-1</sup> in 2080–2100 compared to the mean value over 1985–2005 (Fig. 5a). The parameterization P.OMZ allows for the contributions of high and low O<sub>2</sub> to be isolated and will be analyzed in greater detail in the following sections. N<sub>2</sub>O production via the high-O<sub>2</sub> pathway in P.OMZ decreases on the same order as total

production, by 0.35 TgN yr<sup>-1</sup> in 2080–2100 compared to the present. The N<sub>2</sub>O production in the low-O<sub>2</sub> regions remains almost constant across the experiment. In P.TEMP parameterization, the reduction in N<sub>2</sub>O production is much weaker than in P.OMZ due to the effect of the increasing temperature. N<sub>2</sub>O production decreases by 0.07 TgN yr<sup>-1</sup> in 2080–2100 compared to present (Fig. 5b).

The vast majority of the changes in the N<sub>2</sub>O production in the P.OMZ parameterization is caused by the high-O<sub>2</sub> pathway with virtually no contribution from the low-O<sub>2</sub> pathway (Fig. 5a). As the N<sub>2</sub>O production in P.OMZ parameterization is solely driven by changes in the O<sub>2</sub> consumption (Eq. 2), which in our model is directly linked to export production, the dominance of this pathway implies that the primary driver for the future changes in N<sub>2</sub>O production in our model is the decrease in export of organic matter (CEX). It was simulated to decrease by 0.97 PgC yr<sup>-1</sup> in 2100, and the high degree of correspondence in the temporal evolution of export and N<sub>2</sub>O production in Fig. 5a confirms this conclusion.

The close connection between N<sub>2</sub>O production associated with the high-O<sub>2</sub> pathway and changes in export production is also seen spatially (Fig. 5c), where the spatial pattern of changes in export and changes in N<sub>2</sub>O production are extremely highly correlated (shown by stippling). Most of the small deviations are caused by lateral advection of organic carbon, causing a spatial separation between changes in O<sub>2</sub> consumption and changes in organic matter export.

As there is an almost ubiquitous decrease in export in all of the major oceanic basins except at high latitudes, N<sub>2</sub>O production decreases overall as well. Hotspots of reductions exceeding  $-10 \text{ mgN m}^{-2} \text{ yr}^{-1}$  are found in the North Atlantic and the western Pacific and Indian basins (Fig. 5c). The fewer places where export increases are also the locations of enhanced N<sub>2</sub>O production. For example, a moderate increase of  $3 \text{ mgN m}^{-2} \text{ yr}^{-1}$  is projected in the Southern Ocean, South Atlantic and eastern tropical Pacific. The general pattern of export changes, i.e., decreases in lower latitudes and increases in higher latitudes, is consistent generally with other model projection patterns (Bopp et al., 2013), although there exist very strong model-to-model differences at the more regional scale.

Although the global contribution of the changes in the low-O<sub>2</sub> N<sub>2</sub>O production is small, this is the result of regionally compensating trends. In the model's OMZs, i.e., in the eastern tropical Pacific and in the Bay of Bengal, a significant increase in N<sub>2</sub>O production is simulated in these locations (Fig. 5d), with an increase of more than  $15 \text{ mgN m}^{-2} \text{ yr}^{-1}$ . This increase is primarily driven by the expansion of the OMZs in our model (shown by stippling), while changes in export contribute less. In effect, NEMO-PISCES projects a 20% increase in the hypoxic volume globally, from  $10.2$  to  $12.3 \times 10^6 \text{ km}^3$ , and an increase in the suboxic volume from  $1.1$  to  $1.6 \times 10^6 \text{ km}^3$  in 2100 (Fig. 5e). Elsewhere, the changes in the N<sub>2</sub>O production through the low-O<sub>2</sub> pathway are dominated by the changes in export, thus following the

pattern of the changes seen in the high-O<sub>2</sub> pathway. Overall these changes are negative, and happen to nearly completely compensate for the increase in production in the OMZs, resulting in the near constant global N<sub>2</sub>O production by the low-O<sub>2</sub> production pathway up to year 2100.

#### 4.2.2 Changes in storage of N<sub>2</sub>O

A steady increase in the N<sub>2</sub>O inventory is observed from the present to 2100. The pool of oceanic N<sub>2</sub>O down to 1500 m, i.e., potentially outgassed to the atmosphere, increases by 8.9 TgN from 1985–2005 to year 2100 in P.OMZ, whereas P.TEMP is less sensitive to changes, with an increase of 4.0 TgN for the time period considered (Fig. 6a). The inventory in the upper 1500 m in P.OMZ is 237.0 TgN at present, while in P.TEMP in the same depth band it is 179.8 TgN. This means that the projected changes in the inventory represent an increase of about 4 and 2% in P.OMZ and P.TEMP, respectively.

This increase in storage of N<sub>2</sub>O in the ocean interior shows a homogeneous pattern for P.TEMP, with particular hotspots in the North Pacific, North Atlantic and the eastern boundary currents in the Pacific (Fig. 6b). The spatial variability is more pronounced in P.OMZ (Fig. 6c), related in part to the enhanced production associated with OMZs. Most of the projected changes in storage are associated with shoaling of the mixed layer depth (shown by stippling), suggesting that increase in N<sub>2</sub>O inventories is caused by increased ocean stratification. Enhanced ocean stratification, in turn, occurs in response to increasing sea surface temperatures associated with global warming (Sarmiento et al., 2004).

#### 4.2.3 Effects of the combined mechanisms on N<sub>2</sub>O emissions

The drivers of the future evolution of oceanic N<sub>2</sub>O emissions emerge from the preceding analysis. Firstly, a decrease in the high-O<sub>2</sub> production pathway driven by a reduced organic matter remineralization reduces N<sub>2</sub>O concentrations below the euphotic zone. Secondly, the increased N<sub>2</sub>O inventory at depth is caused by increased stratification and therefore to less efficient transport to the sea–air interface, leading to a smaller N<sub>2</sub>O flux.

The global changes in N<sub>2</sub>O flux, N<sub>2</sub>O production and N<sub>2</sub>O storage for P.OMZ are presented in Fig. 7. Changes in N<sub>2</sub>O flux and N<sub>2</sub>O production are mostly of the same sign in almost all of the oceanic regions, in line with the assumption of nitrification begin the dominant contribution to N<sub>2</sub>O production. Changes in N<sub>2</sub>O production in the subsurface are translated into corresponding changes in N<sub>2</sub>O flux. There is only one oceanic region (subpolar Pacific) where this correlation does not occur. The N<sub>2</sub>O inventory increases in all of the oceanic regions. The increase in inventory is particularly pronounced at low latitudes along the eastern boundary currents in the equatorial and tropical Pacific, Indian Ocean

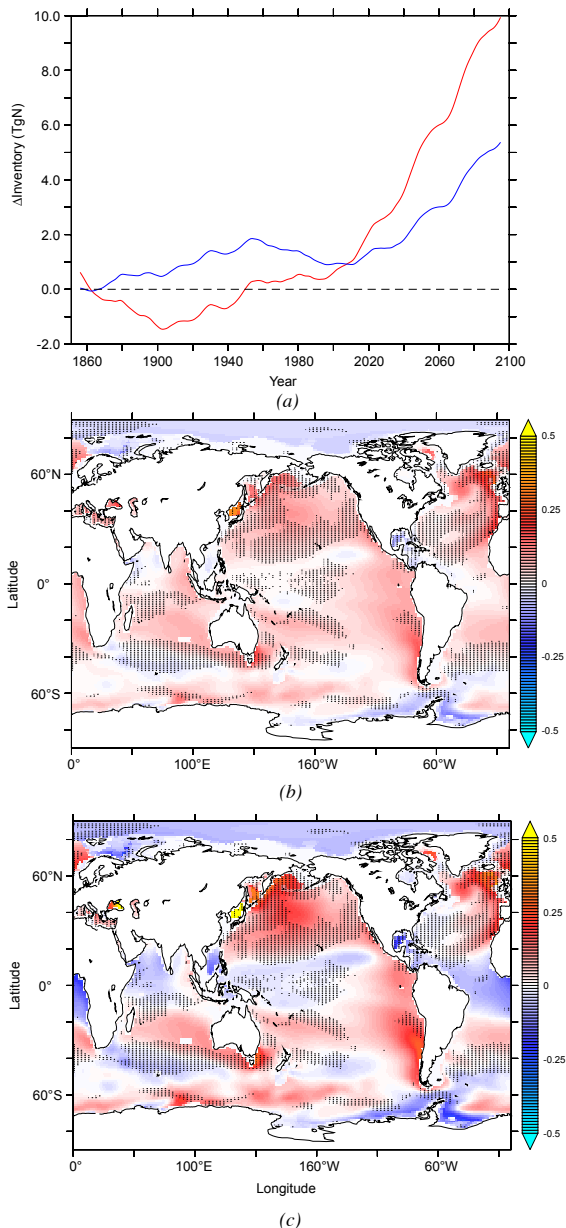


**Figure 6.** (a) Anomalies in N<sub>2</sub>O inventory (in TgN) from 1851 to 2100 in P.TEMP (blue) and P.OMZ (red) using the historical and future RCP8.5 simulations in the upper 1500 m. Change in vertically integrated N<sub>2</sub>O concentration (in mgN m<sup>-2</sup>) in the upper 1500 m using NEMO-PISCES model mean from the averaged 2080–2100 to 1985–2005 time periods in future RCP8.5 and historical scenarios, respectively, in (b) P.TEMP and (c) P.OMZ. Hatched areas indicate regions where the annual mean mixed layer depth is reduced by more than 5 m in 2080–2100 compared to 1985–2005.

and also in smaller quantities in the Atlantic Ocean. Figure 7 shows how the decrease in N<sub>2</sub>O production and increase in N<sub>2</sub>O storage occurs in all oceanic basins.

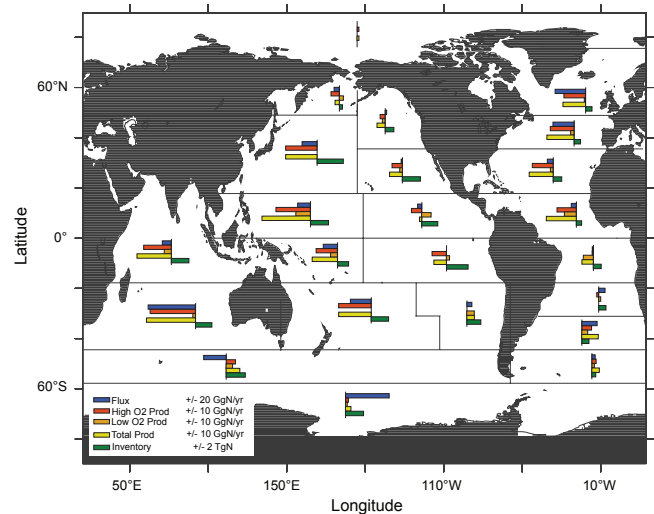


**Figure 7.** Change in the whole water column in N<sub>2</sub>O sea-to-air flux (blue), high-O<sub>2</sub> production pathway (red), low-O<sub>2</sub> production pathway (orange), total N<sub>2</sub>O production (yellow) and N<sub>2</sub>O inventory (green) for P.OMZ from the averaged 2080–2100 to present 1985–2005 averaged time period in the NEMO-PISCES historical and future RCP8.5 simulations (based on Fletcher et al. (2006) oceanic regions).

## 5 Caveats in estimating N<sub>2</sub>O using ocean biogeochemical models

The state variables upon which representation of N<sub>2</sub>O in models rely, i.e., oxygen and export of carbon, are compared to the CMIP5 model ensemble to put our analysis into the context of the current state-of-the-art model capabilities. We focus here our analysis on suboxic waters ( $O_2 < 5 \mu\text{mol L}^{-1}$ ) and export production. Whereas CMIP5 models tend to have large volumes of  $O_2$  concentrations in the suboxic regime, it is not the case for our NEMO-PISCES simulation, which clearly underestimates the volume of low-oxygen waters as compared to the oxygen-corrected World Ocean Atlas 2005 (WOA2005\*) (Bianchi et al., 2012). The fact that NEMO-PISCES forced by IPSL-CM5A-LR is highly oxygenated is confirmed by Fig. 8, where the histogram of the full  $O_2$  spectrum of WOA2005\* and NEMO-PISCES is shown. The  $O_2$  distribution in the model shows a deficient representation of the OMZs, with higher concentrations than those from observations. The rest of the  $O_2$  spectrum is well represented in our model.

The  $O_2$  distribution in the model (Fig. 9) shows a deficient representation of the OMZs, with higher concentrations than those from observations in WOA2005\* and the other CMIP5 models. NEMO-PISCES is therefore biased towards the high  $O_2$  production pathway of N<sub>2</sub>O due to the modeled  $O_2$  fields.

When turning to the export of organic matter, NEMO-PISCES is close to the CMIP5 average value of  $6.9 \text{ PgC yr}^{-1}$ . The overall distribution of export is also very similar to the

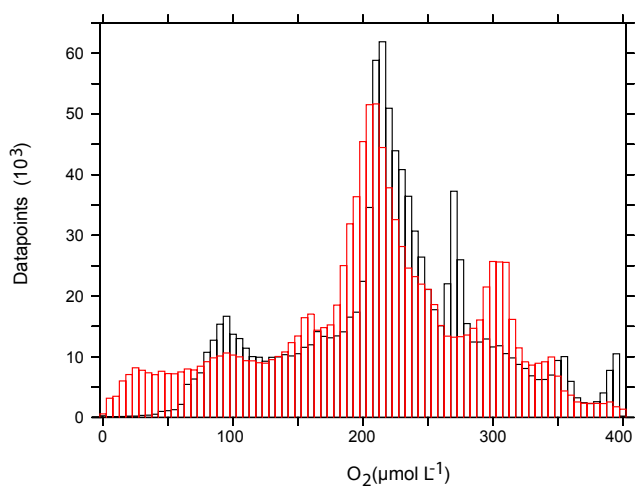


**Figure 8.** Distribution of O<sub>2</sub> concentration in the NEMO-PISCES 1985 to 2005 averaged time period (black) compared to the oxygen-corrected World Ocean Atlas (red) from Bianchi et al. (2012). Interval widths are O<sub>2</sub> concentrations at steps of 5 μmol L<sup>-1</sup>.

CMIP5 model mean, and both show smaller values than those from the data-based estimate of 9.84 PgC yr<sup>-1</sup> from Dunne et al. (2007) (Fig. 9).

The uncertainties derived from present and future model projections can be estimated using the spread in the CMIP5 model projection of export of organic matter and assuming a linear response between nitrification (or export) and N<sub>2</sub>O production in the subsurface, which is assumed to be quickly outgassed to the atmosphere. In NEMO-PISCES, a decrease of 13 % in export leads to a maximum decrease in N<sub>2</sub>O emissions of 12 % in the P.OMZ scenario. Based on results by Bopp et al. (2013), changes in export of carbon span -7 to -18 % in the CMIP5 model ensemble at the end of the 21st century and for RCP8.5. The spread would propagate to a similar range in projected N<sub>2</sub>O emissions across the CMIP5 model ensemble. When these values are applied to present N<sub>2</sub>O emissions of 3.6 TgN yr<sup>-1</sup>, uncertainties are then bracketed between -0.25 and -0.65 TgN yr<sup>-1</sup>.

Regarding the low-O<sub>2</sub> pathway, a similar approach is not that straightforward. Zamora et al. (2012) found that a linear relationship between AOU and N<sub>2</sub>O production might occur even at the OMZ of the eastern tropical Pacific. Zamora et al. (2012) acknowledged the fact that the MEMENTO database includes N<sub>2</sub>O advected from other regions and that mixing could play a relevant role, smoothing the fit between N<sub>2</sub>O and AOU from exponential to linear. However, Zamora et al. (2012) quoting Frame and Casciotti (2010), suggested that regions where an exponential relationship in N<sub>2</sub>O production is present might be rare and that other non-exponential N<sub>2</sub>O production processes might occur. Therefore the plot they presented could describe the actual linear relationship between N<sub>2</sub>O production and oxygen consumption. Based on this hypothesis, we could refer again to

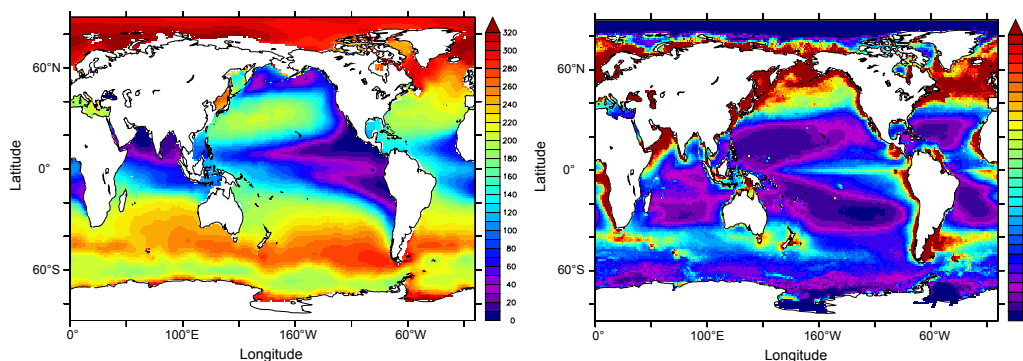
the linear relationship suggested in the high-O<sub>2</sub> and export scenario. However, in this case the CMIP5 model projections of changes in the hypoxic and suboxic volumes differ substantially. Most models project an expansion of the OMZs in the +2 to +16 % range in the suboxic volume (O<sub>2</sub> < 5 μmol L<sup>-1</sup>). There are, however, models that project a slight reduction of 2 %. Spatial variability in projections add to the spread between CMIP5 models. These discrepancies suggest that uncertainties from this spread must be interpreted with caution when estimating potential future N<sub>2</sub>O emissions.

The use of O<sub>2</sub> consumption as a proxy for the actual N<sub>2</sub>O production therefore plays a pivotal role in the uncertainties in N<sub>2</sub>O model estimations. Future model development should aim at the implementation of mechanistic parameterizations of N<sub>2</sub>O production based on nitrification and denitrification rates. Further, in order to determine accurate O<sub>2</sub> boundaries for both N<sub>2</sub>O production and N<sub>2</sub>O consumption at the core of OMZs, additional measurements and microbial experiments are needed. The contribution of the high-O<sub>2</sub> pathway that was considered in this model analysis might be a conservative estimate. Freing et al. (2012) suggested that the high-O<sub>2</sub> pathway could be responsible of 93 % of the total N<sub>2</sub>O production. Assuming that changes in the N<sub>2</sub>O flux are mostly driven by N<sub>2</sub>O production via nitrification, it would suggest a larger reduction in the marine N<sub>2</sub>O emissions in the future. However, the mismatch between NEMO-PISCES and the Nevison et al. (2004) spatial distribution of N<sub>2</sub>O emissions in the western part of the basins suggests that changes in the future might not be as big as those projected in the model in such regions. Changes would be then distributed more homogeneously.

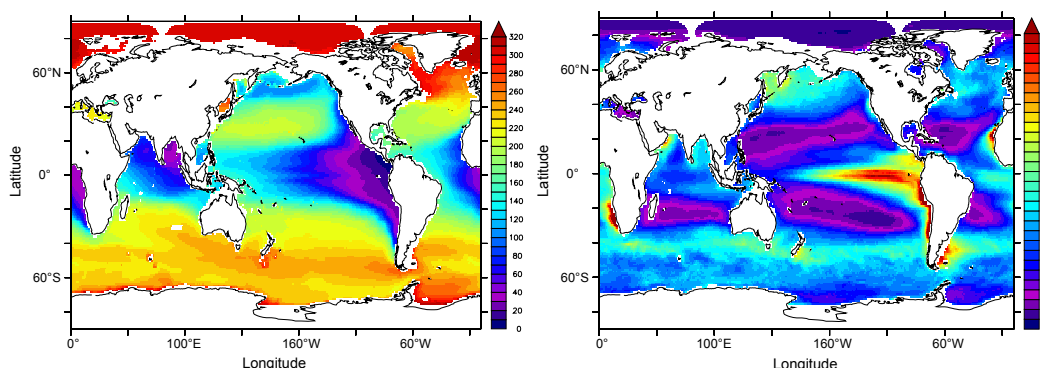
The model assumption neglecting N<sub>2</sub>O production in the upper 100 m avoids one important source of uncertainty in estimating global oceanic N<sub>2</sub>O fluxes. In the case of nitrification occurring in the euphotic layer, our results would be facing a significant uncertainty of at least ±25 % in N<sub>2</sub>O emissions according to Zamora and Oschlies (2014) analysis using the UVic Earth system climate model. Finally, Zamora et al. (2012) observed a higher than expected N<sub>2</sub>O consumption at the core of the OMZ in the eastern tropical Pacific, occurring at an upper threshold of 10 μmol L<sup>-1</sup>. The contribution of OMZs to total N<sub>2</sub>O production remains an open question. N<sub>2</sub>O formation associated with OMZs might be counterbalanced by its own local consumption, leading to the attenuation of the only increasing source of N<sub>2</sub>O attributable to the projected future expansion of OMZs (Steinacher et al., 2010; Bopp et al., 2013).

The combined effect of climate change and ocean acidification has not been analyzed in this study. N<sub>2</sub>O production processes might be altered by the response of nitrification to increasing levels of seawater pCO<sub>2</sub> (Huesemann et al., 2002; Beman et al., 2011). Beman et al. (2011) reported a reduction in nitrification in response to decreasing pH. This result suggests that N<sub>2</sub>O production might decrease beyond what

## a. WOA2005\* and Dunne et al., 2007



## b. CMIP5 model mean



## c. NEMO-PISCES

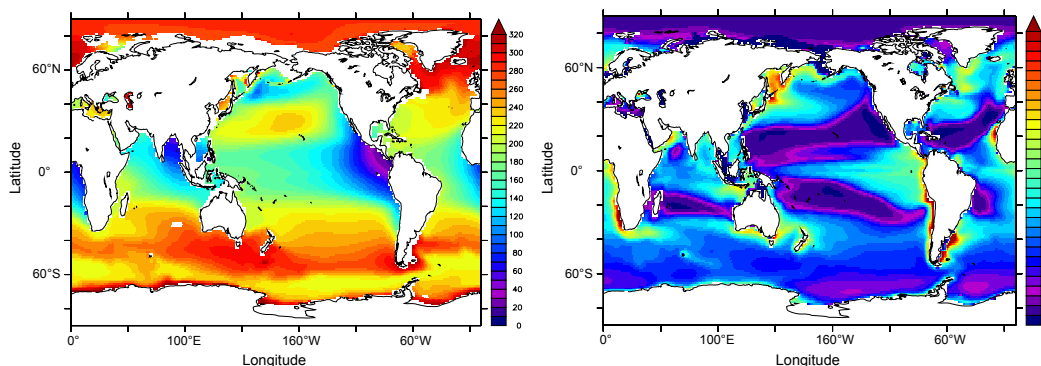


**Figure 9.** Averaged O<sub>2</sub> concentration between 200 and 600 m depth (in  $\mu\text{mol L}^{-1}$ ) (left) and export of carbon (in  $\text{mmol C m}^{-2} \text{d}^{-1}$ ) (right) in (a) WOA2005\* and Dunne et al. (2007), (b) CMIP5 model mean historical simulations over the 1985–2005 time period and (c) NEMO-PISCES for the present 1985–2005 time period.

we have estimated only due to climate change. Conversely, negative changes in the ballast effect could potentially reinforce nitrification at shallow depth in response to less efficient particulate organic carbon export to depth and shallow remineralization (Gehlen et al., 2011). Regarding N<sub>2</sub>O formation via denitrification, changes in seawater pH as a con-

sequence of higher levels of CO<sub>2</sub> might not be substantial enough to change the N<sub>2</sub>O production efficiency, assuming a similar response of marine denitrifiers as reported for denitrifying bacteria in terrestrial systems (Liu et al., 2010). Finally, the C : N ratio in export production (Riebesell et al., 2007) might increase in response to ocean acidification, potentially

leading to a greater expansion of OMZs than simulated here (Oschlies et al., 2008; Tagliabue et al., 2011), and therefore to enhanced N<sub>2</sub>O production associated with the low-O<sub>2</sub> pathway.

Changes in atmospheric nitrogen deposition have not been considered in this study. It has been suggested that, due to anthropogenic activities, the additional amount of reactive nitrogen in the ocean could fuel primary productivity and N<sub>2</sub>O production. Estimates are, however, low, around 3–4 % of the total oceanic emissions (Suntharalingam et al., 2012).

Longer simulation periods could reveal additional effects on N<sub>2</sub>O transport beyond changes in upwelling or meridional transport of N<sub>2</sub>O in the subsurface (Suntharalingam and Sarmiento, 2000) that have been observed in this transient simulation. Long-term responses might include eventual ventilation of the N<sub>2</sub>O reservoir in the Southern Ocean, highlighting the role of upwelling regions as an important source of N<sub>2</sub>O when longer time periods are considered in model projections. Additional studies using other ocean biogeochemical models might also yield alternative values using the same parameterizations. N<sub>2</sub>O production is particularly sensitive to the distribution and magnitude of export of organic matter and O<sub>2</sub> fields defined in models.

## 6 Contribution of future N<sub>2</sub>O to climate feedbacks

Changes in the oceanic emissions of N<sub>2</sub>O to the atmosphere will have an impact on atmospheric radiative forcing, with potential feedbacks on the climate system. Based on the estimated 4 to 12 % decrease in N<sub>2</sub>O sea-to-air flux over the 21st century under RCP8.5, we estimated the feedback factor for these changes as defined by Xu-Ri et al. (2012). Considering the reference value of the preindustrial atmospheric N<sub>2</sub>O concentration of 280 ppb in equilibrium, and its associated global N<sub>2</sub>O emissions of 11.8 TgN yr<sup>-1</sup>, we quantify the resulting changes in N<sub>2</sub>O concentration per degree for the two projected emissions in 2100 using P.TEMP and P.OMZ. The model projects changes in N<sub>2</sub>O emissions of -0.16 and -0.48 TgN yr<sup>-1</sup>, respectively, whereas surface temperature is assumed to increase globally by 3 °C on average according to the physical forcing used in our simulations. These results yield -0.05 and -0.16 TgN yr<sup>-1</sup> K<sup>-1</sup>, or alternatively -1.25 and -3.80 ppb K<sup>-1</sup> for P.TEMP and P.OMZ, respectively. Following Joos et al. (2001) we calculate the feedback factor in equilibrium for projected changes in emissions to be -0.005 and -0.014 W m<sup>-2</sup>K<sup>-1</sup> in P.TEMP and P.OMZ.

Stocker et al. (2013) projected changes in terrestrial N<sub>2</sub>O emissions in 2100 using transient model simulations leading to feedback strengths between +0.001 and +0.015 W m<sup>-2</sup> K<sup>-1</sup>. Feedback strengths associated with the projected decrease in oceanic N<sub>2</sub>O emissions are on the same order of magnitude as those attributable to changes in the terrestrial sources of N<sub>2</sub>O, yet opposite in sign, suggesting a compensation for changes in radiative forcing due to future

increasing terrestrial N<sub>2</sub>O emissions. At this stage, potential balance between land and ocean emissions is to be taken with caution, as it relies of a single model run with constant atmospheric N<sub>2</sub>O.

## 7 Conclusions

Our simulations suggest that anthropogenic climate change could lead to a global decrease in oceanic N<sub>2</sub>O emissions during the 21st century. This maximum projected decrease of 12 % in marine N<sub>2</sub>O emissions for the business-as-usual high-CO<sub>2</sub> emissions scenario would compensate for the estimated increase in N<sub>2</sub>O fluxes from the terrestrial biosphere in response to anthropogenic climate change (Stocker et al., 2013), so that the climate–N<sub>2</sub>O feedback may be more or less neutral over the coming decades.

The main mechanisms contributing to the reduction of marine N<sub>2</sub>O emissions are a decrease in N<sub>2</sub>O production in highly oxygenated waters as well as an increase in ocean vertical stratification that acts to decrease the transport of N<sub>2</sub>O from the subsurface to the surface ocean. Despite the decrease in both N<sub>2</sub>O production and N<sub>2</sub>O emissions, simulations suggest that the global marine N<sub>2</sub>O inventory may increase from 2005 to 2100. This increase is explained by the reduced transport of N<sub>2</sub>O from the production zones to the air–sea interface.

Differences between the two parameterizations used here are more related to biogeochemistry rather than changes in ocean circulation. Despite sharing the high-O<sub>2</sub> N<sub>2</sub>O production pathway, leading to a decrease in N<sub>2</sub>O emissions in both cases, the role of warming in P.TEMP or higher N<sub>2</sub>O yields at low O<sub>2</sub> concentrations in P.OMZ translate into notable differences in the evolution of the two production pathways. However, the dominant effect of changes in stratification in both parameterizations ultimately drives the homogeneous response of the parameterizations considered in model projections in the next century.

The N<sub>2</sub>O production pathways demand, however, a better understanding in order to enable an improved representation of processes in models. The efficiencies of the production processes in response to higher temperatures or increased seawater *p*CO<sub>2</sub> are required. Other effects such as changes in the O<sub>2</sub> boundaries at which nitrification and denitrification occur must be also taken into account. In the absence of process-based parameterizations, N<sub>2</sub>O production parameterizations will still rely on export of organic carbon and oxygen levels. Both need to be improved in global biogeochemical models.

The same combination of mechanisms (i.e., change in export production and ocean stratification) have been identified as drivers of changes in oceanic N<sub>2</sub>O emissions during the Younger Dryas by Goldstein et al. (2003). The N<sub>2</sub>O flux decreased, while the N<sub>2</sub>O reservoir was fueled by longer residence times of N<sub>2</sub>O caused by increased stratification. Other

studies point towards changes in the N<sub>2</sub>O production at the OMZs as the main reason for variations in N<sub>2</sub>O observed in the past (Suthhof et al., 2001). Whether these mechanisms are plausible drivers of changes beyond year 2100 remains an open question that needs to be addressed with longer simulations.

**The Supplement related to this article is available online at doi:10.5194/bg-12-4133-2015-supplement.**

*Acknowledgements.* We thank Cynthia Nevison for providing us the N<sub>2</sub>O sea-to-air flux data set. We thank Annette Kock and Herman Bange for the availability of the MEMENTO database (<https://memento.geomar.de>). We thank Christian Ethé for help analyzing PISCES model drift. Comments by Parvatha Suntharalingam and the three anonymous reviewers significantly improved this paper. Nicolas Gruber acknowledges the support of ETH Zürich. This work was supported by the European Union via the Greencycles II FP7-PEOPLE-ITN-2008, number 238366.

Edited by: F. Joos

## References

- Aumont, O. and Bopp, L.: Globalizing results from ocean in situ iron fertilization studies, *Global Biogeochem. Cy.*, 20, GB2017, doi:10.1029/2005gb002591, 2006.
- Bange, H. W., Rixen, T., Johansen, A. M., Siefert, R. L., Ramesh, R., Ittekkot, V., Hoffmann, M. R., and Andreae, M. O.: A revised nitrogen budget for the Arabian Sea, *Global Biogeochem. Cy.*, 14, 1283–1297, doi:10.1029/1999gb001228, 2000.
- Bange, H. W., Bell, T. G., Cornejo, M., Freing, A., Uher, G., Upstill-Goddard, R. C., and Zhang, G.: MEMENTO: a proposal to develop a database of marine nitrous oxide and methane measurements, *Environ. Chem.*, 6, 195–197, doi:10.1071/en09033, 2009.
- Beman, J. M., Chow, C.-E., King, A. L., Feng, Y., Fuhrman, J. A., Andersson, A., Bates, N. R., Popp, B. N., and Hutchins, D. A.: Global declines in oceanic nitrification rates as a consequence of ocean acidification, *P. Natl. Acad. Sci. USA*, 108, 208–213, doi:10.1073/pnas.1011053108, 2011.
- Bianchi, D., Dunne, J. P., Sarmiento, J. L., and Galbraith, E. D.: Data-based estimates of suboxia, denitrification, and N<sub>2</sub>O production in the ocean and their sensitivities to dissolved O<sub>2</sub>, *Global Biogeochem. Cy.*, 26, GB2009, doi:10.1029/2011gb004209, 2012.
- Bindoff, N., Willebrand, J., Artale, V., Cazenave, A., Gregory, J., Gulev, S., Hanawa, K., Le Quere, C., Levitus, S., Norjiri, Y., Shum, C., Talley, L., and Unnikrishnan, A.: Observations: Oceanic Climate Change and Sea Level, in: *Climate Change 2007: The Physical Science Basis. Contribution of Working Group I to the Fourth Assessment Report of the Intergovernmental Panel on Climate Change*, 2007.
- Bopp, L., Resplandy, L., Orr, J. C., Doney, S. C., Dunne, J. P., Gehlen, M., Halloran, P., Heinze, C., Ilyina, T., Séférian, R., Tjiputra, J., and Vichi, M.: Multiple stressors of ocean ecosystems in the 21st century: projections with CMIP5 models, *Biogeosciences*, 10, 6225–6245, doi:10.5194/bg-10-6225-2013, 2013.
- Butler, J. H., Elkins, J. W., Thompson, T. M., and Egan, K. B.: Tropospheric and dissolved N<sub>2</sub>O of the west pacific and east-indian oceans during the el-nino southern oscillation event of 1987, *J. Geophys. Res.-Atmos.*, 94, 14865–14877, doi:10.1029/JD094iD12p14865, 1989.
- Ciais, P., Sabine, C., Bala, G., Bopp, L., Brovkin, V., Canadell, J., Chhabra, A., DeFries, R., Galloway, J., Heimann, M., Jones, C., Le Quéré, C., Myneni, R. B., Piao, S., and Thornton, P.: Carbon and Other Biogeochemical Cycles, in: *Climate Change 2013: The Physical Science Basis. Contribution of Working Group I to the Fifth Assessment Report of the Intergovernmental Panel on Climate Change*, 2013.
- Cocco, V., Joos, F., Steinacher, M., Frölicher, T. L., Bopp, L., Dunne, J., Gehlen, M., Heinze, C., Orr, J., Oeschler, A., Schneider, B., Segschneider, J., and Tjiputra, J.: Oxygen and indicators of stress for marine life in multi-model global warming projections, *Biogeosciences*, 10, 1849–1868, doi:10.5194/bg-10-1849-2013, 2013.
- Cohen, Y. and Gordon, L. I.: Nitrous-oxide in oxygen minimum of eastern tropical north pacific – evidence for its consumption during denitrification and possible mechanisms for its production, *Deep-Sea Res.*, 25, 509–524, doi:10.1016/0146-6291(78)90640-9, 1978.
- Cohen, Y. and Gordon, L. I.: Nitrous-oxide production in the ocean, *J. Geophys. Res.-Oc. Atm.*, 84, 347–353, doi:10.1029/JC084iC01p00347, 1979.
- Crutzen, P. J.: Influence of nitrogen oxides on atmospheric ozone content, *Q. J. Roy. Meteor. Soc.*, 96, 320–326, doi:10.1002/qj.49709640815, 1970.
- de Wilde, H. P. J. and de Bie, M. J. M.: Nitrous oxide in the Schelde estuary: production by nitrification and emission to the atmosphere, *Mar. Chem.*, 69, 203–216, doi:10.1016/s0304-4203(99)00106-1, 2000.
- Deutsch, C., Brix, H., Ito, T., Frenzel, H., and Thompson, L.: Climate-Forced Variability of Ocean Hypoxia, *Science*, 333, 336–339, doi:10.1126/science.1202422, 2011.
- Dufresne, J. L., Foujols, M. A., Denvil, S., Caubel, A., Marti, O., Aumont, O., Balkanski, Y., Bekki, S., Bellenger, H., Benshila, R., Bony, S., Bopp, L., Braconnot, P., Brockmann, P., Cadule, P., Cheruy, F., Codron, F., Cozic, A., Cugnet, D., de Noblet, N., Duvel, J. P., Ethe, C., Fairhead, L., Fichet, T., Flavoni, S., Friedlingstein, P., Grandpeix, J. Y., Guez, L., Guilyardi, E., Hauglustaine, D., Hourdin, F., Idelkadi, A., Ghattas, J., Jous-saume, S., Kageyama, M., Krinner, G., Labetoulle, S., Lahellec, A., Lefebvre, M. P., Lefevre, F., Levy, C., Li, Z. X., Lloyd, J., Lott, F., Madec, G., Mancip, M., Marchand, M., Masson, S., Meurdesoif, Y., Mignot, J., Musat, I., Parouty, S., Polcher, J., Rio, C., Schulz, M., Swingedouw, D., Szopa, S., Talandier, C., Terray, P., Viovy, N., and Vuichard, N.: Climate change projections using the IPSL-CM5 Earth System Model: from CMIP3 to CMIP5, *Clim. Dynam.*, 40, 2123–2165, doi:10.1007/s00382-012-1636-1, 2013.
- Dunne, J. P., Sarmiento, J. L., and Gnanadesikan, A.: A synthesis of global particle export from the surface ocean and cycling through

- the ocean interior and on the seafloor, *Global Biogeochem. Cy.*, 21, GB4006, doi:10.1029/2006gb002907, 2007.
- Elkins, J. W., Wofsy, S. C., McElroy, M. B., Kolb, C. E., and Kaplan, W. A.: Aquatic sources and sinks for nitrous-oxide, *Nature*, 275, 602–606, doi:10.1038/275602a0, 1978.
- Farias, L., Paulmier, A., and Gallegos, M.: Nitrous oxide and N-nutrient cycling in the oxygen minimum zone off northern Chile, *Deep-Sea Res. Pt. I*, 54, 164–180, doi:10.1016/j.dsr.2006.11.003, 2007.
- Fletcher, S. E. M., Gruber, N., Jacobson, A. R., Gloor, M., Doney, S. C., Dutkiewicz, S., Gerber, M., Follows, M., Joos, F., Lindsay, K., Menemenlis, D., Mouchet, A., Muller, S. A., and Sarmiento, J. L.: Inverse estimates of the oceanic sources and sinks of natural CO<sub>2</sub> and the implied oceanic carbon transport, *Global Biogeochem. Cy.*, 21, GB1010, doi:10.1029/2006gb002751, 2007.
- Frame, C. H. and Casciotti, K. L.: Biogeochemical controls and isotopic signatures of nitrous oxide production by a marine ammonia-oxidizing bacterium, *Biogeosciences*, 7, 2695–2709, doi:10.5194/bg-7-2695-2010, 2010.
- Freing, A., Wallace, D. W. R., Tanhua, T., Walter, S., and Bange, H. W.: North Atlantic production of nitrous oxide in the context of changing atmospheric levels, *Global Biogeochem. Cy.*, 23, GB4015, doi:10.1029/2009gb003472, 2009.
- Freing, A., Wallace, D. W. R., and Bange, H. W.: Global oceanic production of nitrous oxide, *Philos. T. R. Soc. B*, 367, 1245–1255, doi:10.1098/rstb.2011.0360, 2012.
- Gehlen, M., Gruber, N., Gangstø, R., Bopp, L., and Oschlies, A.: Biogeochemical consequences of ocean acidification and feedbacks to the earth system, *Ocean Acidification*, 1, 230–248, 2011.
- Goldstein, B., Joos, F., and Stocker, T. F.: A modeling study of oceanic nitrous oxide during the Younger Dryas cold period, *Geophys. Res. Lett.*, 30, 1092, doi:10.1029/2002gl016418, 2003.
- Goreau, T. J., Kaplan, W. A., Wofsy, S. C., McElroy, M. B., Valois, F. W., and Watson, S. W.: Production of NO<sub>2</sub><sup>-</sup> and N<sub>2</sub>O by nitrifying bacteria at reduced concentrations of oxygen, *Appl. Environ. Microb.*, 40, 526–532, 1980.
- Gruber, N.: Warming up, turning sour, losing breath: ocean biogeochemistry under global change, *Philos. T. R. Soc. A*, 369, 1980–1996, doi:10.1098/rsta.2011.0003, 2011.
- Gruber, N.: The marine nitrogen cycle: Overview of distributions and processes, in: *Nitrogen in the marine environment*, 2nd Edn., 1–50, 2008.
- Gruber, N. and Galloway, J. N.: An Earth-system perspective of the global nitrogen cycle, *Nature*, 451, 293–296, doi:10.1038/nature06592, 2008.
- Huesemann, M. H., Skillman, A. D., and Crecelius, E. A.: The inhibition of marine nitrification by ocean disposal of carbon dioxide, *Mar. Pollut. Bull.*, 44, 142–148, doi:10.1016/s0025-326x(01)00194-1, 2002.
- Jin, X. and Gruber, N.: Offsetting the radiative benefit of ocean iron fertilization by enhancing N<sub>2</sub>O emissions, *Geophys. Res. Lett.*, 30, 2249, doi:10.1029/2003gl018458, 2003.
- Johnston, H.: Reduction of stratospheric ozone by nitrogen oxide catalysts from supersonic transport exhaust, *Science*, 173, 517–522, doi:10.1126/science.173.3996.517, 1971.
- Joos, F., Prentice, I. C., Sitch, S., Meyer, R., Hooss, G., Plattner, G. K., Gerber, S., and Hasselmann, K.: Global warming feedbacks on terrestrial carbon uptake under the Intergovernmental Panel on Climate Change (IPCC) emission scenarios, *Global Biogeochem. Cy.*, 15, 891–907, doi:10.1029/2000gb001375, 2001.
- Keeling, R. F., Koertzing, A., and Gruber, N.: Ocean Deoxygenation in a Warming World, *Annu. Rev. Mar. Sci.*, 2, 199–229, doi:10.1146/annurev.marine.010908.163855, 2010.
- Liu, B., Morkved, P. T., Frostegard, A., and Bakken, L. R.: Denitrification gene pools, transcription and kinetics of NO, N<sub>2</sub>O and N<sub>2</sub> production as affected by soil pH, *Fems Microbiol. Ecol.*, 72, 407–417, doi:10.1111/j.1574-6941.2010.00856.x, 2010.
- Mantoura, R. F. C., Law, C. S., Owens, N. J. P., Burkill, P. H., Woodward, E. M. S., Howland, R. J. M., and Llewellyn, C. A.: Nitrogen biogeochemical cycling in the northwestern indian-ocean, *Deep-Sea Res. Pt. II*, 40, 651–671, 1993.
- Myhre, G., Shindell, D., Bréon, F.-M., Collins, W., Fuglestedt, J., Huang, J., Koch, D., Lamarque, J.-F., Lee, D., Mendoza, B., Nakajima, T., Robock, A., Stephens, G., Takemura, T., and Zhang, H.: Anthropogenic and Natural Radiative Forcing. In: *Climate Change 2013: The Physical Science Basis, Contribution of Working Group I to the Fifth Assessment Report of the Intergovernmental Panel on Climate Change*, 2013.
- Nevison, C., Butler, J. H., and Elkins, J. W.: Global distribution of N<sub>2</sub>O and the Delta N<sub>2</sub>O-AOU yield in the subsurface ocean, *Global Biogeochem. Cy.*, 17, 1119, doi:10.1029/2003gb002068, 2003.
- Nevison, C. D., Weiss, R. F., and Erickson, D. J.: Global oceanic emissions of nitrous-oxide, *J. Geophys. Res.-Oceans*, 100, 15809–15820, doi:10.1029/95jc00684, 1995.
- Nevison, C. D., Lueker, T. J., and Weiss, R. F.: Quantifying the nitrous oxide source from coastal upwelling, *Global Biogeochem. Cy.*, 18, GB1018, doi:10.1029/2003gb002110, 2004.
- Oschlies, A., Schulz, K. G., Riebesell, U., and Schmittner, A.: Simulated 21st century's increase in oceanic suboxia by CO<sub>2</sub>-enhanced biotic carbon export, *Global Biogeochem. Cy.*, 22, GB4008, doi:10.1029/2007gb003147, 2008.
- Prather, M. J., Holmes, C. D., and Hsu, J.: Reactive greenhouse gas scenarios: Systematic exploration of uncertainties and the role of atmospheric chemistry, *Geophys. Res. Lett.*, 39, L09803, doi:10.1029/2012gl051440, 2012.
- Punshon, S. and Moore, R. M.: Nitrous oxide production and consumption in a eutrophic coastal embayment, *Mar. Chem.*, 91, 37–51, doi:10.1016/j.marchem.2004.04.003, 2004.
- Ravishankara, A. R., Daniel, J. S., and Portmann, R. W.: Nitrous Oxide (N<sub>2</sub>O): The Dominant Ozone-Depleting Substance Emitted in the 21st Century, *Science*, 326, 123–125, doi:10.1126/science.1176985, 2009.
- Riebesell, U., Schulz, K. G., Bellerby, R. G. J., Botros, M., Fritsche, P., Meyerhoefer, M., Neill, C., Nondal, G., Oschlies, A., Wohlers, J., and Zoellner, E.: Enhanced biological carbon consumption in a high CO<sub>2</sub> ocean, *Nature*, 450, 545–548, doi:10.1038/nature06267, 2007.
- Sarmiento, J. L., Slater, R., Barber, R., Bopp, L., Doney, S. C., Hirst, A. C., Kleypas, J., Matear, R., Mikolajewicz, U., Monfray, P., Soldatov, V., Spall, S. A., and Stouffer, R.: Response of ocean ecosystems to climate warming, *Global Biogeochem. Cy.*, 18, GB3003, doi:10.1029/2003gb002134, 2004.
- Sarmiento, J. L. and Gruber, N.: *Ocean biogeochemical dynamics*, Princeton University Press, 2006.
- Steinacher, M., Joos, F., Frölicher, T. L., Bopp, L., Cadule, P., Cocco, V., Doney, S. C., Gehlen, M., Lindsay, K., Moore, J. K.,

- Schneider, B., and Segschneider, J.: Projected 21st century decrease in marine productivity: a multi-model analysis, *Biogeosciences*, 7, 979–1005, doi:10.5194/bg-7-979-2010, 2010.
- Stocker, B. D., Roth, R., Joos, F., Spahni, R., Steinacher, M., Zehle, S., Bouwman, L., Xu, R., and Prentice, I. C.: Multiple greenhouse-gas feedbacks from the land biosphere under future climate change scenarios, *Nature Climate Change*, 3, 666–672, doi:10.1038/nclimate1864, 2013.
- Suntharalingam, P. and Sarmiento, J. L.: Factors governing the oceanic nitrous oxide distribution: Simulations with an ocean general circulation model, *Global Biogeochem. Cy.*, 14, 429–454, doi:10.1029/1999gb900032, 2000.
- Suntharalingam, P., Sarmiento, J. L., and Toggweiler, J. R.: Global significance of nitrous-oxide production and transport from oceanic low-oxygen zones: A modeling study, *Global Biogeochem. Cy.*, 14, 1353–1370, doi:10.1029/1999gb900100, 2000.
- Suntharalingam, P., Buitenhuis, E., Le Quere, C., Dentener, F., Nevison, C., Butler, J. H., Bange, H. W., and Forster, G.: Quantifying the impact of anthropogenic nitrogen deposition on oceanic nitrous oxide, *Geophys. Res. Lett.*, 39, L07605, doi:10.1029/2011gl050778, 2012.
- Suthhof, A., Ittekkot, V., and Gaye-Haake, B.: Millennial-scale oscillation of denitrification intensity in the Arabian Sea during the late Quaternary and its potential influence on atmospheric N<sub>2</sub>O and global climate, *Global Biogeochem. Cy.*, 15, 637–649, doi:10.1029/2000gb001337, 2001.
- Tagliabue, A., Bopp, L., and Gehlen, M.: The response of marine carbon and nutrient cycles to ocean acidification: Large uncertainties related to phytoplankton physiological assumptions, *Global Biogeochem. Cy.*, 25, GB3017, doi:10.1029/2010gb003929, 2011.
- Takahashi, T., Broecker, W. S., and Langer, S.: Redfield ratio based on chemical-data from isopycnal surfaces, *J. Geophys. Res.-Oceans*, 90, 6907–6924, doi:10.1029/JC090iC04p06907, 1985.
- Tiedje, J. M.: Ecology of denitrification and dissimilatory nitrate reduction to ammonium, *Biology of Anaerobic Microorganisms*, 717, 179–244, 1988.
- Wanninkhof, R.: Relationship between wind-speed and gas-exchange over the ocean, *J. Geophys. Res.-Oceans*, 97, 7373–7382, doi:10.1029/92jc00188, 1992.
- Weiss, R. F. and Price, B. A.: Nitrous-oxide solubility in water and seawater, *Mar. Chem.*, 8, 347–359, doi:10.1016/0304-4203(80)90024-9, 1980.
- Westley, M. B., Yamagishi, H., Popp, B. N., and Yoshida, N.: Nitrous oxide cycling in the Black Sea inferred from stable isotope and isotopomer distributions, *Deep-Sea Res. Pt. II*, 53, 1802–1816, doi:10.1016/j.dsr2.2006.03.012, 2006.
- Xu-Ri, Prentice, I. C., Spahni, R., and Niu, H. S.: Modelling terrestrial nitrous oxide emissions and implications for climate feedback, *New Phytol.*, 196, 472–488, 2012.
- Yoshida, N., Morimoto, H., Hirano, M., Koike, I., Matsuo, S., Wada, E., Saino, T., and Hattori, A.: Nitrification rates and N-15 abundances of N<sub>2</sub>O and NO<sub>3</sub><sup>-</sup> in the western north pacific, *Nature*, 342, 895–897, doi:10.1038/342895a0, 1989.
- Zamora, L. M. and Oschlies, A.: Surface nitrification: A major uncertainty in marine N<sub>2</sub>O emissions, *Geophys. Res. Lett.*, 41, 4247–4253, doi:10.1002/2014gl060556, 2014.
- Zamora, L. M., Oschlies, A., Bange, H. W., Huebert, K. B., Craig, J. D., Kock, A., and Löscher, C. R.: Nitrous oxide dynamics in low oxygen regions of the Pacific: insights from the MEMENTO database, *Biogeosciences*, 9, 5007–5022, doi:10.5194/bg-9-5007-2012, 2012.
- Zehr, J. P. and Ward, B. B.: Nitrogen cycling in the ocean: New perspectives on processes and paradigms, *Appl. Environ. Microb.*, 68, 1015–1024, doi:10.1128/aem.68.3.1015-1024.2002, 2002.